https://doi.org/10.31436/iiumej.v25i2.3240

EFFECT OF INCORPORATING CELLULOSE NANOFIBERS AND LEMONGRASS ESSENTIAL OIL IN POLYVINYL ALCOHOL-POLYETHYLENE GLYCOL/GLYCERIN HYDROGEL FOR WOUND DRESSING

NUR HUDA SYAZWANI JAFRI[1], DZUN NORAINI JIMAT[1*], WAN MOHD FAZLI WAN NAWAWI[1], YUSILAWATI AHMAD NOR[1], AZURA AMID[2]

[1]Department of Chemical Engineering and Sustainability, Faculty of Engineering, International Islamic University Malaysia, P.O Box 10, 50728, Kuala Lumpur, Malaysia

[2]International Institute for Halal Research and Training, International Islamic University Malaysia, P. O Box 10, 50728, Kuala Lumpur, Malaysia

**Corresponding author: jnoraini@iium.edu.my*

(Received: 27 March 2024; Accepted: 27 June 2024; Published online: 15 July 2024)

ABSTRACT: Hydrogels attract increased interest as wound dressings due to their biomimetic properties, creating a moist environment conducive to natural wound healing. In this study, a PVA-PEG/gly-CNF-LG hydrogel incorporating cellulose nanofibers (CNF) and lemongrass essential oil (LG) into the polyvinyl alcohol-polyethylene glycol/glycerin (PVA-PEG/gly) hydrogel via the freeze-thaw method was developed. The addition of CNFs and LG aimed to improve the physicochemical and antibacterial aspects of the hydrogel. Optimal hydrogel composition, determined through response surface methodology (RSM) and central composite design (CCD), consisted of 3.5% (w/v) CNFs and 3% (v/v) LG concentrations, resulting in an optimal moisture retention capability (MRC) of 37.69 ± 0.54%. The optimized PVA-PEG/gly-CNF-LG demonstrated impressive characteristics: a swelling capacity of 176.89 ± 1.56%, a gel fraction of 78.89 ± 0.42%, and a porosity of 47.51 ± 0.53%. FESEM images revealed the relatively porous nature of PVA-PEG/gly-CNF-LG hydrogels. Furthermore, the hydrogel exhibited excellent resistance against S. aureus and B. subtilis bacteria, along with notable tensile properties of 1.44 MPa. These findings underscore the promising attributes of the PVA-PEG/gly-CNF-LG hydrogel, positioning it as a versatile and effective wound-healing dressing with significant antimicrobial properties.

ABSTRAK: Hidrogel mendapat perhatian ramai sebagai pembalut luka di sebabkan oleh ciri-ciri biomimik, di mana menghasilkan persekitaran lembab yang baik bagi penyembuhan luka secara semula jadi. Kajian ini, mencadangkan hidrogel PVA-PEG/gly-CNF-LG yang mengandungi selulosa nanofiber (CNF) dan minyak pati serai (LG) dalam hidrogel polivenil alkohol-polietilin glikol/gliserin (PVA-PEG/gly) melalui kaedah beku-cair. Penambahan CNFs dan LG diperlukan bagi memperbaiki aspek fisiokimia dan antibakterial hidrogel. Komposisi optimal hidrogel, dibentuk melalui kaedah respons permukaan (RSM) dan reka bentuk komposit pusat (CCD), mengandungi 3.5% (w/v) CNFs dan 3% (v/v) kepekatan LG, menghasilkan kemampuan retensi kelembapan optimal (MRC) sebanyak 37.69 ± 0.54%. Kadar optimum PVA-PEG/gly-CNF-LG menunjukkan ciri-ciri yang menarik: iaitu kapasiti pembengkakan sebanyak 176.89 ± 1.56%, pecahan gel sebanyak 78.89 ± 0.42%, dan keliangan 47.51 ± 0.53%. Imej FESEM menunjukkan sifat keliangan semula jadi hidrogel PVA-PEG/gly-CNF-LG. Tambahan, hidrogel memiliki rintangan tinggi terhadap bakteria S. aureus dan B. subtilis, sejajar dengan ciri-ciri ketara tegangan 1.44 MPa. Dapatan kajian ini penting bagi ciri-ciri hidrogel yang berpotensi besar seperti PVA-PEG/gly-CNF-LG,

menjadikannya serba guna dan berkesan sebagai balutan penyembuhan luka dengan ciri-ciri antimikrob yang ketara.

KEYWORDS: *Cellulose Nanofibers, Glycerin, Lemongrass essential oil, Polyethylene glycol, Polyvinyl alcohol*

1. INTRODUCTION

Polyvinyl alcohol (PVA), a synthetic polymer, shows significant promise for wound dressing applications due to its hydrophilic nature and high biocompatibility [1–3]. PVA-based hydrogel dressings demonstrate exceptional moisture retention ability by mimicking natural tissue conditions, thereby establishing and maintaining the moist environment necessary for faster healing processes [4]. Moreover, PVA hydrogels are easily synthesized by adjusting their structure, composition, and interactions to meet specific requirements. They can also be combined with bioactive agents such as antibiotics and growth factors to enhance therapeutic effectiveness. These combined attributes render PVA hydrogels versatile and valuable materials in the field of wound care and other medical applications [2, 5].

Despite their beneficial properties, PVA hydrogels have several drawbacks that limit their use as wound dressings. Their relatively weak mechanical properties make them susceptible to breakage and deformation, thus failing to adequately support and protect wounds [2, 5]. Reduced flexibility contributes to the challenge of PVA hydrogel dressings adhering properly to wounds and surrounding skin. Additionally, the rapid hydration of PVA hydrogels can lead to the production of stiff, dry dressings that hinder their ability to maintain a sufficiently hydrated environment, which is crucial for accelerating wound healing [6, 7].

To enhance wound dressing performance and provide effective wound care, it is essential to modify the hydrogel composition to mitigate the drawbacks of PVA hydrogel wound dressings [8, 9]. Various components can be blended together in a unified or single polymeric matrix to create materials with desired properties [10, 11]. Polyethylene glycol (PEG) is renowned for its remarkable hydrophilic properties, significantly enhancing the water retention and absorption capacity of hydrogel formulations when incorporated into the hydrogel matrix to promote wound healing. This feature is crucial for preventing the production of rigid and dry hydrogels [8, 12]. Additionally, PEG has low toxicity and is highly biocompatible, making it safe for use in contact with biological tissue. This makes it a common polymer choice in wound dressing applications [2].

The inclusion of glycerin in hydrogel formulation is advantageous due to its excellent humectant and moisturizing characteristics [6, 13]. Glycerin enhances the hydrating action of PEG when added to PVA hydrogel by attracting and retaining water molecules within the hydrogel matrix. This feature is vital to maintain the proper moisture content of the wound dressing and prevent it from drying out [13]. Glycerin can also improve the flexibility and elasticity of PVA hydrogel dressings, allowing them to better conform to the shape of wounds, ensuring proper adherence, and maximizing the healing process [13].

Cellulose nanofibers (CNFs) are fibrous materials with nanoscale dimensions. Besides being lightweight, CNFs exhibit outstanding mechanical properties, making them highly desirable for reinforcement in wound dressings [14, 15]. CNFs serve as reinforcing agents that help strengthen the hydrogel structure, improving the structural integrity of hydrogels. This feature is vital for forming durable hydrogel dressings resistant to degradation and deformation [15, 16]. CNFs can be derived from empty fruit bunches (EFB), the major biomass waste of

palm oil mills. Due to its high cellulose content, EFB can be utilized as a feedstock for large-scale nanocellulose production, providing a sustainable alternative [15].

Lemongrass essential oil (LG) exhibits potent antibacterial properties due to bioactive compounds such as citral and geraniol, which can combat a wide range of pathogens. Incorporating LG into the hydrogel formulation imparts antibacterial properties to the hydrogel dressings, reducing the risk of infection and accelerating wound healing [17, 18]. Moreover, LG possesses other therapeutic qualities that promote wound healing, such as anti-inflammatory and antioxidant actions, enhancing the effectiveness of hydrogel wound dressings [17, 19].

There are several methods for making hydrogels, including various crosslinking techniques such as physical, radiation, and chemical methods [20]. The most commonly employed technique is the freeze-thaw method due to its ease of synthesis, cost-effectiveness, and environmentally friendly characteristics. This method does not use chemicals, thereby avoiding toxicity and leaching problems caused by chemical crosslinking. It also enables the production of hydrogels with tailored properties [21].

This study aimed to investigate the properties of polyvinyl alcohol-polyethylene glycol/glycerin (PVA-PEG/gly) hydrogels incorporated with cellulose nanofibers (CNFs) and lemongrass essential oil (LG). This hydrogel, referred to as PVA-PEG/gly-CNF-LG, utilizes central composite design (CCD) within response surface methodology (RSM) to optimize CNF and LG concentrations to achieve maximum moisture retention capability (MRC) of the hydrogel. The optimized hydrogel compositions are evaluated specifically for their swelling properties, gel fraction, and porosity. Additionally, morphological analysis is performed using field emission scanning electron microscopy (FESEM), while Fourier transform infrared spectroscopy (FTIR) is used to analyze functional groups within the hydrogel structure. Furthermore, the antibacterial activity and mechanical strength of the hydrogel are determined via the disc diffusion method and tensile testing, respectively.

2. MATERIALS AND METHODS

2.1 Materials

Dimethyl sulfoxide (DMSO; ≥99.5%) and glycerin (≥99.5%) were provided by R&M Chemical Co., Ltd. Polyethylene glycol (PEG; MW 3350) and polyvinyl alcohol (PVA; MW 89,000-98,000; 99% hydrolyzed) were obtained from Sigma-Aldrich (St. Louis, MO, USA). Luria-Bertani (LB) agar and broth (MILLER) were purchased from Sigma-Aldrich, and tetracycline hydrochloride was sourced from Fisher Scientific, UK. Lemongrass essential oil (LG) from the Soul brand was supplied by BF1 Cosmetic Co., Ltd (Kuala Lumpur, Malaysia).

Empty fruit bunches (EFB) from Kilang Sawit FELCRA Maran in Pahang, Malaysia, were processed for cellulose nanofiber (CNF) extraction. EFB underwent cutting, crushing into small particles using a mini grinder and sieving to produce fine powders (0.5 to 2 mm). Fibers were then heated in distilled water at 80 °C, stirred for 1 h, dried overnight at 40 °C until they reached a constant weight, and stored in airtight containers. The chemicals utilized for CNF extraction were laboratory-grade and sourced from Sigma-Aldrich, USA. These include oxalic acid dihydrate ($C_2H_2O_4$) (≥ 99%), choline chloride ($C_6H_{14}CINO$) (≥ 98%), 98% sodium hydroxide pellets (NaOH), and 35% hydrogen peroxide (H_2O_2). All chemicals used in this research were of analytical grade and underwent no further purification.

2.2. Extracting CNF from Empty Fruit Bunches

The extraction of CNFs from EFB followed the method described by Asem et al. with several modifications [22]. Approximately 30 g of EFB fibers were boiled in a 4% (w/v) NaOH solution at 85 °C with a solid-to-solvent ratio of 1:30 and continuously stirred for 2 hours. The fibers were then filtered, washed with deionized water until reaching a neutral pH, and subsequently bleached for 3 h at 95 °C using a 1:1 mixture of deionized water and H_2O_2. This bleaching process was repeated three times. After bleaching, the fibers underwent multiple rinses with distilled water until the wash pH reached neutrality. They were then filtered using a vacuum pump to acquire solid residues. Subsequently, these solid residues were dried at 50 °C until reaching a constant weight. The obtained solid residue is referred to as EFB cellulose [22].

Next, the EFB cellulose was dissolved in a DES mixture of choline chloride-oxalic acid dehydrates (ChCl-OAD) at a DES molar ratio of 1:2 with a fiber-to-solution ratio of 1:10 (w/v), and heated to 90 °C for 90 min with continuous stirring. The cellulose suspensions obtained were centrifuged repeatedly at 9,000 rpm for 15 min in deionized water until reaching a neutral pH. They were then subjected to ultrasonication (using FisherbrandTM Model 705 Sonic Dismembrator) for 2 h at 80% amplitude (280 W). The CNF suspension underwent a 15-minute centrifugation at 10,000 rpm to isolate the CNFs from the liquid. The collected CNFs were then stored in an airtight container in a refrigerator set at 4 °C.

2.3 Synthesis of PVA-PEG/gly-CNF-LG Hydrogel

The hydrogel was prepared following the method outlined by Altaf et al. with modifications [6]. Initially, a 20% (v/v) DMSO solution was prepared by mixing it with deionized water at 45 °C for 15 min. Subsequently, a 15% (w/v) PVA solution in DMSO was prepared and heated to 90 °C for 1 h with constant stirring until translucent. Once complete PVA dissolution was achieved, 6% (w/v) PEG was gradually added, and the resulting solution was agitated for 1 h at 90 °C to form a homogenized PVA-PEG polymeric solution. Glycerin (gly) at a concentration of 4% (w/v) was then incrementally added, heated to 95 °C, and vigorously agitated for 1 h.

CNFs and LG were blended into the polymeric solution at various compositions according to the central composite design (CCD) to optimize their concentrations. Similarly, CNFs were dissolved in deionized water at various concentrations and heated for 30 min at 95 °C with mechanical stirring, aligning with the optimization of the hydrogel composition. Then, the CNFs solution was mixed with the PVA-PEG/glycerin polymer solution in a 1:1 ratio and stirred at 95 °C for 1 h. Afterward, LG was added to the polymeric solution at different concentrations and stirred continuously for 30 min at a constant temperature, aligning with hydrogel composition optimization. The resulting solution was transferred into a petri dish and cooled to room temperature to solidify into a gel. Finally, the hydrogel underwent three cycles of freezing (18 h at -20 °C) and thawing (2 h at ambient temperature). The resulting hydrogel was designated as PVA-PEG/gly-CNF-LG hydrogel.

2.4 Experimental Design and Optimization

Experimental design, data processing, optimization, and modeling were conducted using Design-Expert® Version 12 software (Stat-Ease Inc., Minneapolis, MN). Response surface methodology (RSM) was employed to identify the optimal hydrogel composition for maximum moisture retention capability (MRC) through central composite design (CCD). CNF and LG concentrations were chosen as independent variables, while MRC served as the response or dependent variable. Table 1 provides the details of the CCD design.

https://doi.org/10.31436/iiumej.v25i2.3240

Table 1. CCD design of each variable with its corresponding ranges.

Variables	Levels		
	-1	0	+1
CNF concentration [A] (% w/v)	1	3.5	6
LG concentration [B] (% v/v)	1	3.0	5

Each independent variable was assessed at three levels (-1, 0, +1), resulting in 13 experimental runs with five replications, including center points, four axial points, and four cube points. The response, measured moisture retention capability (MRC), was fitted to a second-order polynomial model. Model validity was assessed through analysis of variance (ANOVA) at a confidence level of 95%. Three-dimensional surface plots were employed to illustrate the effects and interactions of variables on responses. In the validation study, experimental results falling within the 95% confidence interval (*CI*) were utilized to confirm the projected optimum hydrogel formulation by RSM.

2.5 Field Emission Scanning Electron Microscope

The surface morphology of the produced hydrogel was examined using a field emission scanning electron microscope (FESEM) (Model Supra 55VP, Carl Zeiss AG, Germany). The sample was coated with platinum prior to microscopic examination. The hydrogel's microstructure was observed under standard conditions at a magnitude of 50 kV.

2.6 Fourier Transform Infrared Spectroscopy

The functional groups and chemical bonds present in the produced hydrogels were analyzed using a Spectrum RX Fourier Transform Infrared (FTIR) spectrophotometer (PerkinElmer, Norwalk, USA). The FTIR spectra of the samples were recorded with a resolution of 4 cm^{-1} within the spectral transmittance region spanning from 400 to 4000 cm^{-1}.

2.7 Gel Fraction

The hydrogel samples were cut into uniform pieces (2 cm width × 2 cm length) with a thickness of 0.3 cm. Subsequently, they underwent drying for 24 hours in a 40°C oven until reaching a constant weight (W_o). Next, they were submerged in deionized water and allowed to swell for 48 h at room temperature until equilibrium swelling was achieved, effectively eliminating any soluble materials. Afterward, the sample was dried at 40 °C for 24 h to attain a stable weight (W_e). The percentage of gel fraction (GF) was evaluated using Equation 1.

$$\% \text{ GF} = (W_e/W_o) \times 100 \quad (1)$$

Here, W_o is the weight of the dried hydrogel, and W_e is the weight of the swollen hydrogels.

2.8 Swelling Behavior Measurement

The hydrogels, with dimensions of 2 cm length, 2 cm width, and 0.3 cm thickness, were prepared to assess their swelling properties. Initially, the initial weight (W_d) of the hydrogels was recorded before soaking them in deionized water for 24 h at room temperature. Afterwards, the swollen samples were retrieved, and excess water was removed by blotting with filter paper. They were then weighed again (W_s). Equation 2 was utilized to calculate the swelling ratio.

$$\text{Swelling ratio } (\%) = \frac{(W_s - W_d)}{W_d} \times 100 \quad (2)$$

https://doi.org/10.31436/iiumej.v25i2.3240

Here, W_d represents the weight of the dried hydrogels, and W_s represents the weight of the swollen hydrogels.

2.9 Moisture Retention Capability

The hydrogel samples, standardized to dimensions of 2 cm in width, 2 cm in length, and 0.3 cm in thickness, were initially weighed, placed in a 40 °C oven for 6 h, and then weighed again. The moisture retention capability (MRC) was calculated using Equation 3.

$$\text{MRC}\ (\%) = (W_f/W_i) \times 100 \quad (3)$$

where, W_i denotes the starting weight of hydrogel samples, whereas W_f signifies the weight after heating at 40 °C for 6 h.

2.10 Hydrogel Membrane Porosity

The hydrogel samples, standardized to dimensions of 2 cm in width, 2 cm in length, and 0.3 cm in thickness, were immersed in ethanol for 24 h until saturated at room temperature. Measurements were taken before and after ethanol absorption to determine the hydrogel membrane porosity (φ) using Equation 4.

$$\varphi\ (\%) = (W_f - W_i)/(\rho V_f - \rho V_i) \times 100 \quad (4)$$

where, W_i and W_f represent the mass of samples before and after ethanol absorption, respectively. Additionally, V_i and V_f are the ethanol volume before and subsequent absorption, respectively. ρ is the density of ethanol at room temperature.

2.11 Zeta Potential Measurement

The zeta potential of hydrogel samples was analyzed using the Zetasizer Nanoparticle Analyzer (Nano ZS, Model ZEN 3600, Malvern Instrument Ltd., UK). Dynamic light scattering (DLS) was employed to measure samples at 25 °C, utilizing Helium-Neon (He-Ne) lasers emitting a 633 nm wavelength and a 176° backscatter detector.

2.12 Antibacterial Activity Assessment

The antibacterial activity was assessed using a disc diffusion method inspired by Altaf et al. (2021) with modifications to evaluate the hydrogel's effectiveness against bacteria. Various strains, including *Bacillus subtilis (B. subtilis)*, *Staphylococcus aureus (S. aureus)*, *Escherichia coli (E. coli)*, and *Salmonella enteritidis (S. enteritidis)*, were employed. A loopful of bacterial cells from stock cultures was transferred into sterile Luria-Bertani (LB) broth and incubated at 37 °C for 24 h to produce an inoculum of 10^6 CFU/mL.

Hydrogel samples (1 cm × 1 cm, 0.3 cm thickness) were placed on LB agar plates containing bacteria, sterilized with UV light for 20 min, and then incubated for 24 h at 37 °C. The diameter of the inhibition zones measured bacterial growth inhibition, and Vernier calipers were used to quantify the zone of inhibition after removing the agar plates from the incubator. Tetracycline hydrochloride and DMSO served as positive and negative controls, respectively. All apparatus used in the antibacterial test were autoclaved to prevent contamination.

The hydrogel samples (measuring 1 cm × 1 cm, with a thickness of 0.3 cm) were placed on LB agar plates containing bacteria, sterilized with UV light for 20 min, and then incubated for 24 h at 37 °C. After removing the agar plates from the incubator, the diameter of the inhibition zones, which indicated bacterial growth inhibition, was measured using Vernier calipers. Tetracycline hydrochloride and DMSO served as positive and negative controls,

respectively. All apparatus used in the antibacterial test were autoclaved to prevent contamination.

2.12 Mechanical Testing

The initial gap between the sample and grips was adjusted to 40 mm. Tensile testing was conducted to assess the mechanical properties of hydrogels following ASTM D638 standards, employing the electronic universal testing machine (Instron® Model 3366, UK) equipped with a 10 kN load cell. Initially, the hydrogels were shaped into standard dumbbell forms with dimensions of 6 mm in height, 40 mm in diameter, and 3 mm in thickness. The tensile tests were performed with 90% compression at a strain rate of 10 mm min^{-1}. The initial gap between the sample and grips was set to 40 mm.

3. RESULTS AND DISCUSSION

3.1 Statistical Optimization of Hydrogel Composition

The study examined the synergistic impact of CNFs and LG concentrations on the MRC of the hydrogel utilizing RSM with a CCD, as detailed in Table 2. Thirteen experimental runs were carried out for hydrogel compositions to evaluate the influence of these two factors on the MRC of the hydrogel.

Table 2. CCD for hydrogel composition.

Run	CNF concentration [A] (% w/v)	LG concentration [B] (% v/v)	MRC (%)
1	3.5	5	31.03
2	1	1	27.20
3	6	3	32.25
4	3.5	3	37.03
5	6	5	25.46
6	3.5	3	37.68
7	3.5	1	32.46
8	6	1	30.89
9	3.5	3	36.36
10	1	3	32.74
11	3.5	3	37.36
12	1	5	30.00
13	3.5	3	37.69

Mean data values were employed to formulate a second-order polynomial equation, resulting in a regression equation to determine the optimal MRC within the experimental limits. The linear equation for MRC (Y) depicted the experimental data, as presented in Equation 5.

$$Y = +15.233 + 5.700A + 8.327B - 0.412AB - 0.651A^2 - 1.204B^2 \quad (5)$$

In this context, Y represents the MRC, while A and B denote the independent variables for CNFs and LG concentrations, respectively.

Positive coefficients indicated that the chosen independent variables, CNFs and LG concentrations, positively influenced the hydrogel's MRC. This suggested that within the specified experimental range, higher concentrations of CNFs and LG led to increased MRC of the hydrogel, highlighting a favorable correlation between these variables and the desired outcome [7, 23].

https://doi.org/10.31436/iiumej.v25i2.3240

The model's effectiveness and statistical significance were assessed through variance analysis (ANOVA), confirming its adequacy, as delineated in Table 3. ANOVA aided in validating the constructed model by maintaining the hierarchical structure and identifying and eliminating irrelevant interactions [6]. The model's probability value (p-value) had to be below 0.05 to be considered significant [7, 24].

Table 3. ANOVA of hydrogel formulation.

Source	Sum of squares	DF	Mean square	F-value	p-value	
Model MRC (Y)	196.60	5	39.32	108.76	<0.0001	Significant
A-CNF concentration	0.2993	1	0.2993	0.8278	0.3932	
B-LG concentration	2.75	1	2.75	7.60	0.0282	
AB	16.93	1	16.93	46.84	0.0002	
A^2	45.68	1	45.68	126.35	<0.0001	
B^2	64.08	1	64.08	177.25	<0.0001	
Residual	2.53	7	0.3615	-	-	
Lack of Fit	1.30	3	0.4344	1.42	0.3617	Not significant
Pure Error	1.23	4	0.3069	-	-	
Cor Total	199.13	12	-	-	-	
R^2	0.9873		Adequate Precision		28.988	
Adjusted R^2	0.9878		C.V. %		1.83	
Predicted R^2	0.9463		Standard Deviation %		0.6013	

Table 3 indicated that the model demonstrated significance with a low p-value ($p < 0.0001$) and an F-value of 108.76. The likelihood of noise resulting in such a high F-value was only 0.01%. All terms (B, AB, A^2, and B^2) exhibited lower p-values, designating them as significant model terms, except for term A (CNFs concentration). The regression coefficients R^2, adjusted R^2, and estimated R^2 aided in evaluating the model's fit to the experimental data, with values closer to 1 indicating a superior fit [25]. The model achieved a substantial R^2 of 0.9873, ensuring an accurate fit to the experimental data. The predicted R^2 (0.9463) closely matched the adjusted R^2 (0.9878), suggesting that the insignificant term had minimal impact on the model [3]. The insignificant lack of fit affirmed the model's adequacy, demonstrating a robust correlation between process variables and output response [25].

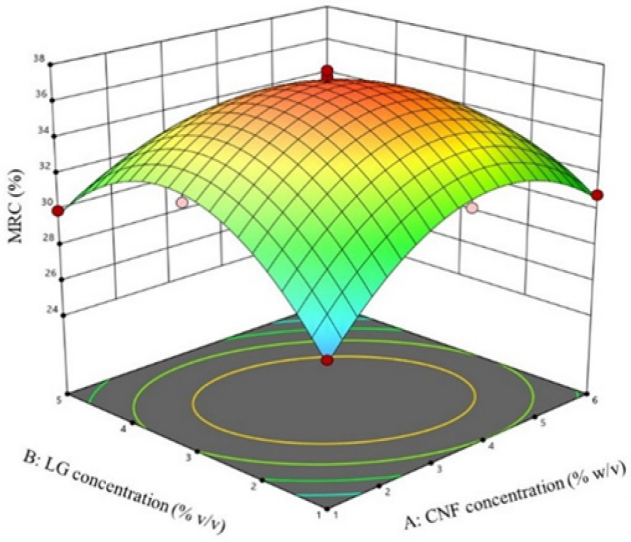

Figure 1. The response surface graph showed the impact of CNF and LG concentrations on the MRC of the hydrogel.

Fig. 1 illustrates the influence of CNFs and LG concentrations on the hydrogel's MRC through three-dimensional response surface graphs. Circular shapes represent insignificant interactions, whereas elliptical forms indicate more pronounced interactions [25, 26]. The downward-facing curve and symmetrical shapes confirm a robust correlation between CNF and LG concentrations and the hydrogel's MRC [26].

Through RSM optimization, the ideal hydrogel composition was determined to be 3.5% (w/v) CNF and 3% (v/v) LG concentrations, resulting in the highest MRC of 37.69%. Building upon this optimal formulation, a validation experiment yielded a hydrogel with an MRC of 37.82 ±0.54%, which closely aligns with the predicted MRC value of 37.06%. This validation underscores the efficacy of the RSM model for hydrogel formulation [7]. Hydrogels must exhibit substantial moisture retention capabilities, essential for creating and maintaining a moist environment that fosters optimal healing processes and ensures effective wound dressing [27, 28].

3.2 Swelling Behavior Assessment

The ability of the hydrogel to absorb a significant volume of wound exudates and biological fluids serves as a criterion for assessing its effectiveness as a wound dressing [29, 30]. As depicted in Fig. 2b, the swelling capacities of various hydrogels are presented. The optimized PVA-PEG/gly-CNF-LG hydrogel displayed the highest swelling capacity at 176.89 ± 1.56%, surpassing that of PVA and PVA-PEG/gly hydrogels, which measured 154.4 ± 0.46% and 143.24 ± 1.66%, respectively. A previous study on PVA/PEG hydrogels indicated a lower swelling capacity than the PVA-PEG/gly-CNF-LG hydrogel [2]. Moreover, a hydrogel with a swelling capacity exceeding 100% is typically considered a highly absorbent polymer [7].

PVA and PVA-PEG/gly-CNF-LG hydrogels displayed distinct characteristics attributed to differences in their compositions. For example, due to its flexible nature, the PVA-PEG/gly-CNF-LG hydrogel demonstrated the ability to bend or stretch without breaking. Conversely, PVA hydrogel typically exhibited a solid-like structure that was rigid and susceptible to deformation. The flexible attributes the PVA-PEG/gly-CNF-LG hydrogel exhibited were attributed to the incorporation of moisture-retaining components such as PEG and glycerin into the hydrogel matrix [8, 31].

3.3 Gel Fraction Measurement

Gel fraction (GF) is a critical parameter that can be used to quantify the degree of crosslinking among the constituents employed in producing hydrogels within their polymeric matrix [6]. The GFs of hydrogels produced in this study are depicted in Fig. 2a. The optimized PVA-PEG/gly-CNF-LG hydrogel exhibited the highest GF of 78.89 ± 0.42%. In comparison, the GFs for PVA and PVA-PEG/gly hydrogels were 36.99 ± 0.34% and 58.06 ± 1.65%, respectively. The PVA-PEG/gly-CNF-LG hydrogel demonstrated a higher gel fraction than an earlier study with the PVA/starch hydrogel containing clove oils, where the gel fraction was reported at 64% [6].

For the optimized PVA-PEG/gly-CNF-LG hydrogel, the heightened gel fraction validates successful cross-linking interactions among its constituents, including PVA, PEG, glycerin, CNFs, and LG. This intricate cross-linking resulted in a robust and cohesive three-dimensional polymer network within the hydrogel matrix, significantly enhancing its mechanical strength, structural integrity, and ability to maintain shape and functionality when used as a wound dressing [8, 32].

https://doi.org/10.31436/iiumej.v25i2.3240

PEG, being hydrophilic, exhibited a significant affinity for water molecules. Its hydrophilic nature enhanced hydrogels' moisture retention and absorption capabilities when incorporated into their structures [2]. Additionally, glycerin complemented PEG's hydrating effect by permitting substantial water molecules to enter and exit the hydrogel matrix, thus ensuring a moist environment conducive to rapid wound healing [13]. As glycerin and PEG facilitated the penetration of water molecules into the hydrogel matrix, the interaction between the water molecules and polymer chains became stronger due to increased physical entanglements and contact between them. This resulted in complex and interconnected hydrogel structure formation, consequently elevating the gel fraction [13]. Moreover, integrating CNFs as reinforcement to strengthen the hydrogel structure led to the creation of new pores and channels within the hydrogel matrix, thereby enhancing its structural integrity and moisture absorption capabilities [33, 34].

3.4 Hydrogel Porosity

The porosities of hydrogels produced in this study are depicted in Fig. 2. Optimal porosities were achieved by the PVA-PEG/gly-CNF-LG hydrogel at 47.51 ± 0.53%, surpassing those of the PVA-PEG/gly hydrogel at 35.02 ± 1.34% and the PVA hydrogel at 27.42 ± 0.65%. Maintaining a porosity between 30% and 40% for hydrogel dressings is recommended to balance preserving a moist wound environment and effectively absorbing fluids and exudates [6, 8]. This range ensures that the dressing can effectively manage wound moisture without drying out the wound or being overwhelmed by exudates.

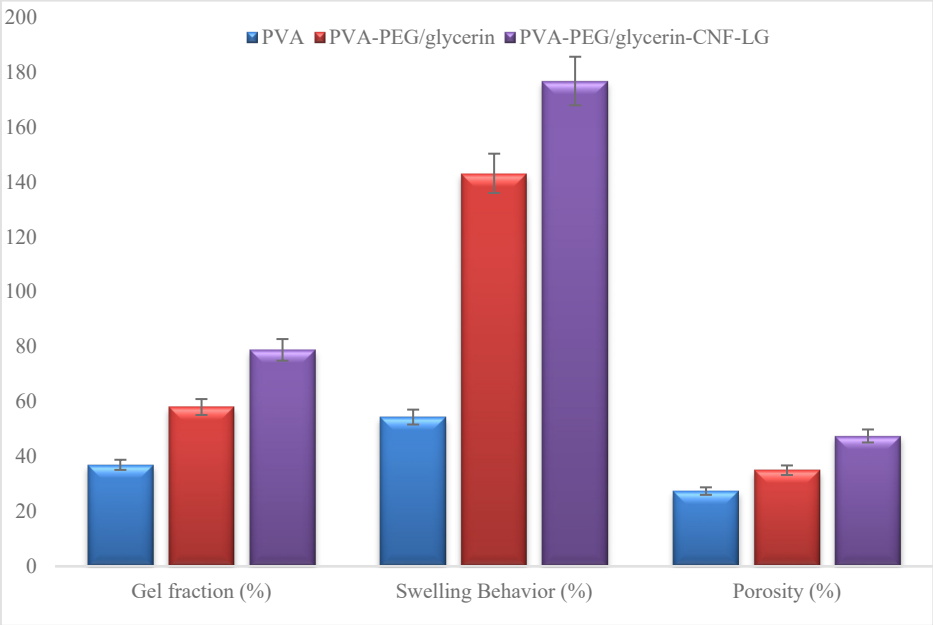

Figure 2. Physical properties, (a) gel fraction, (b) swelling behavior, and (c) porosity for PVA, PVA-PEG/gly, and PVA-PEG/gly-CNF-LG hydrogels.

However, a porosity level of 47.51% for the PVA-PEG/gly-CNF-LG hydrogel was deemed acceptable and beneficial. Higher porosity enabled greater fluid absorption, particularly advantageous for heavily exuding wounds, while also aiding in maintaining an optimal moist environment for healing. If the hydrogel maintained good structural integrity, it could still offer effective wound coverage and protection [6]. Conversely, a lack of porosity in hydrogel dressing hampered gaseous exchange and fluid absorption, potentially impeding the healing process. Additionally, excessive porosity leading to overabsorption of fluids could

result in issues such as wound drying and inadequate drainage, thereby causing discomfort to the patient [4]. Therefore, ensuring an appropriate porosity level in hydrogels was crucial to enhancing their performance as dressing materials [35].

3.5 Examination of Hydrogel Morphology

The microstructural properties of hydrogel wound dressings significantly influenced gaseous exchange, swelling capacity, and, consequently, the rate of wound healing [3]. Figure 4 presented the resulting FESEM images, revealing distinct morphologies between the PVA-PEG/gly hydrogel and the PVA-PEG/gly-CNF-LG hydrogel.

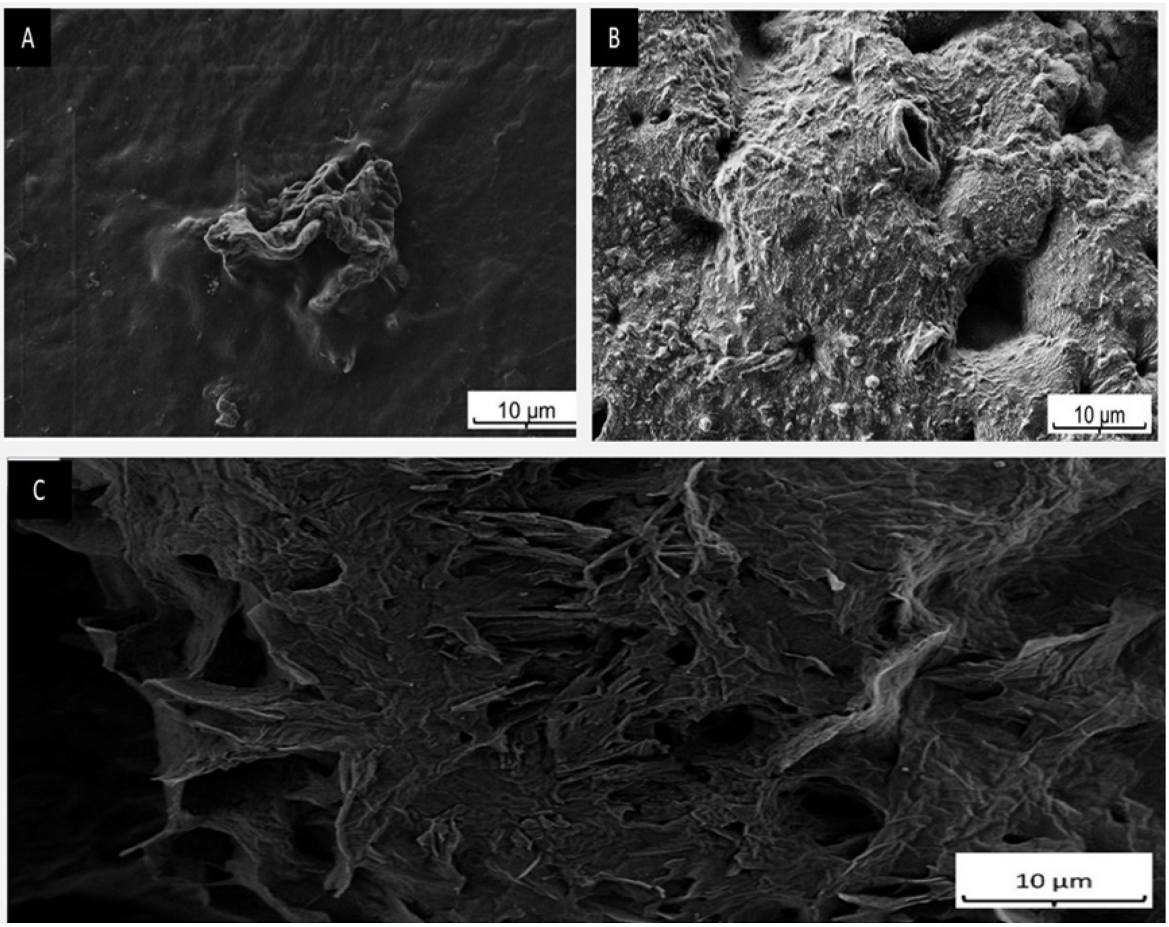

Figure 3. FESEM images (a) PVA; (b) PVA-PEG/gly; and (c) PVA-PEG/gly-CNF-LG hydrogels at 50 kV magnification.

In Fig. 3, the pure PVA hydrogel exhibited a rigid, non-porous bulk structure. In contrast, the PVA-PEG/gly-CNF-LG hydrogel displayed a highly porous structure. The fibrillar morphology of the PVA-PEG/gly hydrogel became more pronounced with incorporating CNF, consistent with previous findings [3, 7]. Surface ripples and bumps emerged on the PVA-PEG/gly hydrogel structure, attributed to changes in physical properties and surface tension resulting from including PEG and glycerin. Both compounds, being hydrophilic, enhanced the hydrogel's water-absorption capacity [8, 9]. Their introduction increased the hydrogel's moisture content, leading to expansion and swelling. However, this expansion could cause surface irregularities due to non-uniform water distribution and the formation of localized tension zones [6, 9]. These areas with varying tension resulted in ripples and bumps on the

https://doi.org/10.31436/iiumej.v25i2.3240

hydrogel's surface, visually representing the modified structure and increased moisture content [36]. Such characteristics were desirable in applications like wound dressings and drug delivery systems, emphasizing the hydrogel's ability to absorb and retain water [33, 37].

Adding CNFs, PEG, and glycerin to the PVA-PEG/gly-CNF hydrogel increased surface roughness and irregularities. CNFs created a fibrous network, enhancing mechanical strength and surface undulations. PEG and glycerin enhanced hydrophilicity, promoting greater water absorption and swelling [38]. This elevated moisture content resulted in uneven expansion and surface irregularities due to varying water distribution. These combined effects increased roughness, providing advantages in wound dressing materials by improving cell adhesion and tissue integration for enhanced wound healing. Additionally, the irregularities offered more sites for drug loading and release in drug delivery systems, making the hydrogel a valuable platform for controlled drug delivery [38, 39].

3.6 FTIR Analysis

Fig. 4 depicts Fourier transform infrared (FTIR) images of hydrogels, revealing the presence of hydroxyl (-OH) groups responsible for the hydrogel's water-binding ability. The peak strength observed in the hydrogel's FTIR findings directly correlated with its capacity to absorb water and wound exudates [7]. The hydrogen bonding interaction between the hydroxyl groups of PVA and PEG was evident in the -OH bond vibrations at around 1100-1450 cm^{-1}, with prominent peaks at 1438 cm^{-1} and 2916 cm^{-1} indicating stretching vibrations of -CH and CH2, respectively. These vibrations were primarily attributed to PVA [2, 3]. Additionally, the presence of C=O and C=C bonds in PVA, PEG, and LG was demonstrated by peaks at 1600 and 1800 cm^{-1} [6, 40].

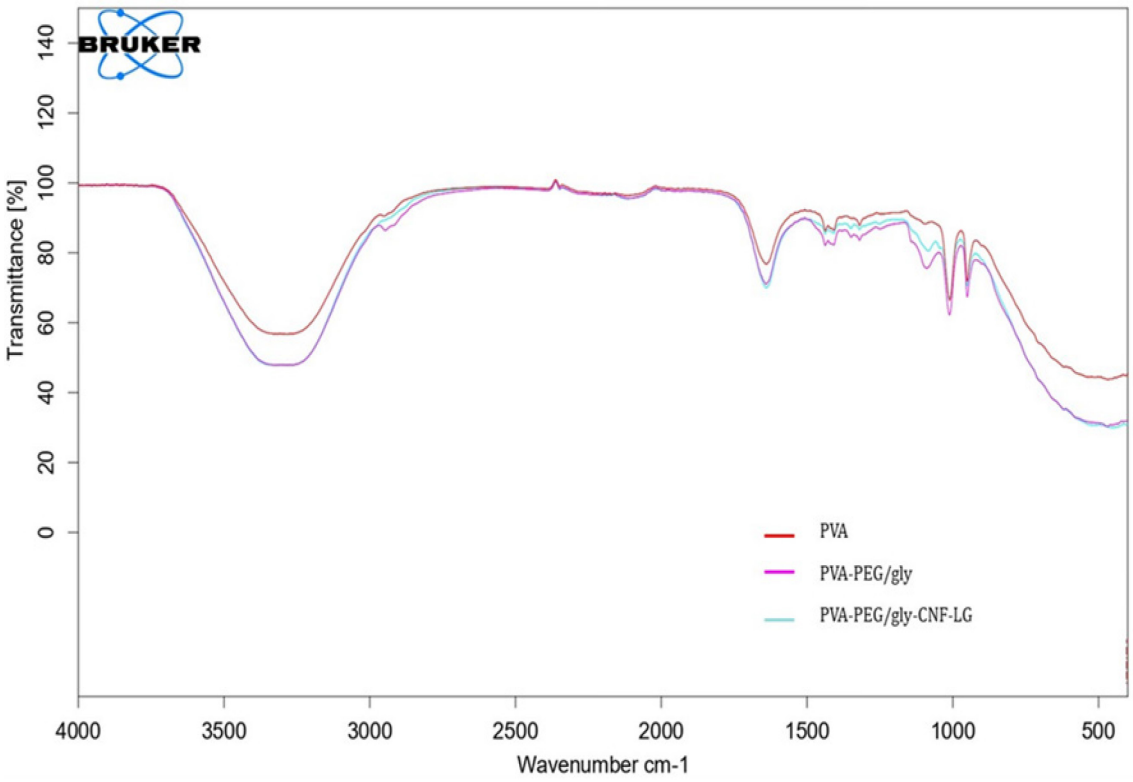

Figure 4. FTIR image of hydrogels. (a) PVA; (b) PVA-PEG/gly; and (c) PVA-PEG/gly-CNF-LG

The broadest band observed between 3200 and 3400 cm^{-1} in each spectrum indicated the stretching vibration of -OH bonds in PVA, PEG, and glycerin, a consistent feature across all hydrogel compositions [8, 13]. The presence of cellulose in the hydrogel was confirmed by a peak at 1044 cm^{-1}, signifying C-O and C-H stretching vibrations [41]. Noteworthy peaks at lower wavenumbers included the -CH2- group in the aliphatic PVA chain, resulting in C-H bonds with deformation vibrations in the 1430–1450 cm^{-1} region [42]. The stretching vibrations of C-H from PEG and glycerin caused a visible peak between 2916 and 2359 cm^{-1} in the PVA-PEG/glycerin spectra [3, 8]. Importantly, the FTIR spectra of the PVA hydrogel did not exhibit these peaks.

3.7 Zeta Potential Measurement

Zeta potential measurement served as a valuable method for evaluating the surface charge of nanoparticles within colloidal solutions [3]. In the case of the PVA-PEG/gly-CNF-LG hydrogel, a zeta potential of -15.9 mV was observed. This zeta potential implied a high degree of stability in the solution, reducing the possibility of coagulation or aggregation, which was vital for using this hydrogel as dressing material [6, 8]. A hydrogel with a negative zeta potential indicated a negatively charged surface, which repelled negatively charged particles or cells, lowering the potential risk of adhesion or fouling, a crucial property in biomedical applications [3].

In contrast, PVA and PVA-PEG/gly hydrogels recorded zeta potentials of -33.5 mV and -38.8 mV, respectively. The increasing pattern of absolute zeta potential values from PVA to PVA-PEG/gly hydrogels implied that the surface charge became greater after the inclusion of PEG and glycerin into the hydrogel structure, resulting in better stability by preventing adhesion or aggregation [6, 9]. The larger zeta potential was deemed beneficial in biomedical applications as it signified fewer interactions with proteins or cells, preventing fouling or undesirable interactions for forming stable colloids, which were essential to sustain consistent dispersion and functionality [12].

3.8 Antibacterial Testing

The disc diffusion method was applied to examine the antibacterial efficiency of the produced PVA-PEG/gly-CNF-LG hydrogel against several bacterial strains. The results showed that the PVA-PEG/gly-CNF-LG hydrogel was effective against gram-positive bacteria, as indicated by inhibition zones measuring 3.5 ± 0.2 cm for *B. subtilis* and 2.5 ± 0.3 cm for *S. aureus*. Citral, a key lemongrass (LG) component, is recognized for its efficacy against gram-positive bacteria [40]. However, no inhibition zone was observed against *E. coli* and *S. enteritidis*, indicating the absence of antibacterial effects of the PVA-PEG/gly-CNF-LG hydrogel against gram-negative bacteria. Detailed findings on the hydrogel's antibacterial activity were summarized in Table 4, alongside the control groups for comparison.

Table 4. Antibacterial effectiveness of hydrogels.

Compound	Inhibition zone diameter (cm)			
	E. coli	*B. subtilis*	*S. aureus*	*S. enteritidis*
PVA-PEG/gly-CNF-LG	NA	3.5 ± 0.2	2.5 ± 0.3	NA
Tetracycline hydrochloride (+ve control)	2.7± 0.4	3.2 ± 0.1	2.3 ± 0.1	2.8± 0.3
Dimethyl sulfoxide (- ve control)	NA	NA	NA	NA

The varying antibacterial outcomes observed in the PVA-PEG/gly-CNF-LG hydrogel against distinct bacterial strains—where it showed no efficacy against *E. coli* and *S. enteritidis* but demonstrated effectiveness against *B. subtilis* and *S. aureus*—may have stemmed from various factors. Initially, the inclusion of LG in the hydrogel formulation likely played a significant role. LG contained bioactive compounds like citral, which are known for their antimicrobial properties against specific bacteria. *B. subtilis* and *S. aureus* are gram-positive bacteria with a single-cell membrane, making them generally more susceptible to antimicrobial agents found in LG [43]. On the other hand, *E. coli* and *S. enteritidis* are gram-negative bacteria with a double cell membrane that acts as a barrier, rendering them less susceptible to the penetration of certain antimicrobial agents [18, 43].

3.9 Mechanical Characteristics of Hydrogel

Improving the tensile strength of hydrogels was crucial for ensuring their efficacy as wound dressings. Tensile strength assesses a material's capacity to withstand stretching or pulling forces without fracturing [44]. The tensile stress-strain graph of hydrogels, as depicted in Fig. 5 and considering comparable thickness, was utilized to evaluate their tensile characteristics.

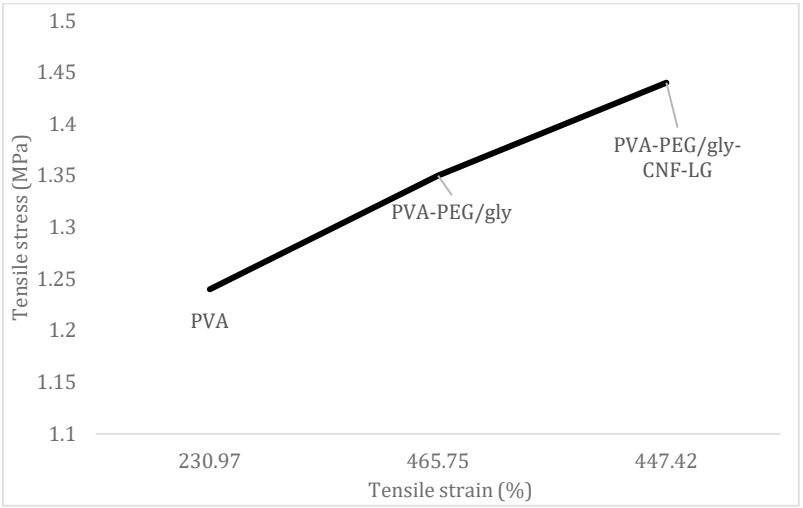

Figure 5. Tensile stress against strain graph for produced hydrogel.

The PVA hydrogel exhibited a tensile strength of 1.24 MPa. Meanwhile, the tensile strength increased to 1.35 MPa after incorporating 4% (w/v) glycerin and 6% (w/v) of PEG into the PVA hydrogel to yield the PVA-PEG/gly hydrogel. This enhancement was attributed to the increased number of crosslinking sites within the three-dimensional polymer network as a result of glycerin and PEG's hydrophilic nature, which created hydrogen bonds to fortify the hydrogel structure, resulting in the increased tensile properties of the hydrogels [3, 8]. Subsequently, the tensile strength further increased after incorporating 3.5% (w/v) CNF and 3% (v/v) LG, resulting in a tensile strength of 1.44 MPa for the PVA-PEG/gly-CNF-LG hydrogel.

4. CONCLUSION

Incorporating PEG, glycerin, CNF, and LG into the polymeric matrix of PVA was conducted via the freeze-thaw method to produce the PVA-PEG/gly-CNF-LG hydrogel for wound dressing application. The highest MRC of 37.69 ± 0.54% was attained for the PVA-PEG/gly-CNF-LG hydrogel at the optimum hydrogel composition with concentrations of 3.5%

(w/v) CNFs and 3% (v/v) LG. The optimized PVA-PEG/glycerin-CNF-LG exhibited impressive characteristics, including a 176.89 ± 1.56% swelling capacity, 78.89 ± 0.42% gel fraction, and 47.51 ± 0.53% porosity. FESEM analysis showed that the produced hydrogel was highly porous, with empty void spaces within its structure. The FTIR spectra showcased the effective cross-linking of the PVA-PEG/glycerin polymeric network with CNF and LG. Antibacterial investigations revealed the resilience of the PVA-PEG/gly-CNF-LG hydrogel against *S. aureus* and *B. subtilis*. Additionally, it demonstrated outstanding tensile characteristics, reaching 1.44 MPa. These findings collectively highlight the promising potential of the optimized PVA-PEG/glycerin-CNF-LG hydrogel as a wound dressing material.

ACKNOWLEDGEMENT

The author would like to thank the Biochemical Laboratory Department of Chemical Engineering & Sustainability, International Islamic University Malaysia, for the laboratory facilities.

REFERENCES

[1] Lin SP, Lo KY, Tseng TN, Liu JM, Shih TY, Cheng KC (2019) Evaluation of PVA/dextran/chitosan hydrogel for wound dressing. Cellular Polymers 38:15–30

[2] Ahmed AS, Mandal UK, Taher M, Susanti D, Jaffri JM (2018) PVA-PEG physically cross-linked hydrogel film as a wound dressing: experimental design and optimization. Pharm Dev Technol 23:751–760

[3] Li Y, Zhu C, Fan D, Fu R, Ma P, Duan Z, Li X, Lei H, Chi L (2019) A Bi-Layer PVA/CMC/PEG Hydrogel with Gradually Changing Pore Sizes for Wound Dressing. Macromol Biosci. https://doi.org/10.1002/mabi.201800424

[4] Baghaie S, Khorasani MT, Zarrabi A, Moshtaghian J (2017) Wound healing properties of PVA/starch/chitosan hydrogel membranes with nano Zinc oxide as antibacterial wound dressing material. J Biomater Sci Polym Ed 28:2220–2241

[5] Butylina S, Geng S, Laatikainen K, Oksman K (2020) Cellulose Nanocomposite Hydrogels: From Formulation to Material Properties. Front Chem. https://doi.org/10.3389/fchem.2020.00655

[6] Altaf F, Niazi MBK, Jahan Z, Ahmad T, Akram MA, safdar A, Butt MS, Noor T, Sher F (2021) Synthesis and Characterization of PVA/Starch Hydrogel Membranes Incorporating Essential Oils Aimed to be Used in Wound Dressing Applications. J Polym Environ 29:156–174

[7] Rahmi D, Paramadina S, Anjelika M, Widjajanti R (2020) Optimized swelling properties of hydrogels based on poly(vinyl alcohol)-carrageenan. AIP Conf Proc. https://doi.org/10.1063/5.0001098

[8] Cui L, Tong W, Zhou H, Yan C, Chen J, Xiong D (2021) PVA-BA/PEG hydrogel with bilayer structure for biomimetic articular cartilage and investigation of its biotribological and mechanical properties. J Mater Sci 56:3935–3946

[9] Chen K, Liu J, Yang X, Zhang D (2017) Preparation, optimization and property of PVA-HA/PAA composite hydrogel. Materials Science and Engineering C 78:520–529

[10] Carating CAM, Rosales RNM, Bongao HC, Magdaluyo ER (2019) Polyvinyl alcohol hydrogel reinforcement of cellulose and silica nanoparticles for wound healing application. In: Key Eng Mater. Trans Tech Publications Ltd, pp 23–28

[11] Butylina S, Geng S, Oksman K (2016) Properties of as-prepared and freeze-dried hydrogels made from poly(vinyl alcohol) and cellulose nanocrystals using freeze-thaw technique. Eur Polym J 81:386–396

[12] Abu Ghalia M, Dahman Y (2015) Radiation crosslinking polymerization of poly (vinyl alcohol) and poly (ethylene glycol) with controlled drug release. Journal of Polymer Research. https://doi.org/10.1007/s10965-015-0861-9

[13] Bialik-Was K, Pluta K, Malina D, Barczewski M, Malarz K, Mrozek-Wilczkiewicz A (2021) The effect of glycerin content in sodium alginate/poly(Vinyl alcohol)-based hydrogels for

wound dressing application. Int J Mol Sci. https://doi.org/10.3390/ijms222112022
[14] Ali MASS, Jimat DN, Nawawi WMFW, Sulaiman S (2022) Antibacterial, Mechanical and Thermal Properties of PVA/Starch Composite Film Reinforced with Cellulose Nanofiber of Sugarcane Bagasse. Arab J Sci Eng 47:5747–5754
[15] Gea S, Indra, Muis Y, Panindia N, Hutapea YA (2019) Preparation of polyvinyl alcohol/cellulose nano fiber nanocomposite isolated from empty oil palm fruit bunches. IOP Conf Ser Mater Sci Eng. https://doi.org/10.1088/1757-899X/553/1/012041
[16] Liu R, Dai L, Si C, Zeng Z (2018) Antibacterial and hemostatic hydrogel via nanocomposite from cellulose nanofibers. Carbohydr Polym 195:63–70
[17] Naik MI, Fomda BA, Jaykumar E, Bhat JA (2010) Antibacterial activity of lemongrass (Cymbopogon citratus) oil against some selected pathogenic bacterias. Asian Pac J Trop Med 3:535–538
[18] Fatunmibi OO, Njoku IS, Asekun OT, Ogah JO (2023) Chemical composition, antioxidant and antimicrobial Activity of the essential oil from the leaves of Cymbopogon citratus.
[19] Shah G, Shri R, Panchal V, Sharma N, Singh B, Mann AS (2011) Scientific basis for the therapeutic use of Cymbopogon citratus, stapf (Lemon grass). J Adv Pharm Technol Res 2:3–8
[20] Entezam M, Daneshian H, Nasirizadeh N, Khonakdar HA, Jafari SH (2017) Hybrid Hydrogels Based on Poly(vinyl alcohol) (PVA)/Agar/Poly(ethylene glycol) (PEG) Prepared by High Energy Electron Beam Irradiation: Investigation of Physico-Mechanical and Rheological Properties. Macromol Mater Eng. https://doi.org/10.1002/mame.201600397
[21] Figueroa-Pizano MD, Vélaz I, Martínez-Barbosa ME (2019) A freeze-thawing method to prepare chitosan-poly(Vinyl alcohol) hydrogels without crosslinking agents and diflunisal release studies. Journal of Visualized Experiments. https://doi.org/10.3791/59636
[22] Asem M, Noraini Jimat D, Huda Syazwani Jafri N, Mohd Fazli Wan Nawawi W, Fadhillah Mohamed Azmin N, Firdaus Abd Wahab M (2023) Entangled cellulose nanofibers produced from sugarcane bagasse via alkaline treatment, mild acid hydrolysis assisted with ultrasonication. Journal of King Saud University - Engineering Sciences 35:24–31
[23] Douard L, Bras J, Encinas T, Belgacem MN (2021) Natural acidic deep eutectic solvent to obtain cellulose nanocrystals using the design of experience approach. Carbohydr Polym. https://doi.org/10.1016/j.carbpol.2020.117136
[24] Rezvanian M, Ahmad N, Mohd Amin MCI, Ng SF (2017) Optimization, characterization, and in vitro assessment of alginate-pectin ionic cross-linked hydrogel film for wound dressing applications. Int J Biol Macromol 97:131–140
[25] Thakur M, Sharma A, Ahlawat V, Bhattacharya M, Goswami S (2020) Process optimization for the production of cellulose nanocrystals from rice straw derived α-cellulose. Mater Sci Energy Technol 3:328–334
[26] Bacha EG (2022) Response Surface Methodology Modeling, Experimental Validation, and Optimization of Acid Hydrolysis Process Parameters for Nanocellulose Extraction. S Afr J Chem Eng 40:176–185
[27] Alven S, Nqoro X, Aderibigbe BA (2020) Polymer-based materials loaded with curcumin for wound healing applications. Polymers (Basel) 12:1–25
[28] Shitole AA, Raut PW, Khandwekar A, Sharma N, Baruah M (2019) Design and engineering of polyvinyl alcohol based biomimetic hydrogels for wound healing and repair. Journal of Polymer Research. https://doi.org/10.1007/s10965-019-1874-6
[29] Singh BR, Singh V, Singh RK (2016) Antimicrobial activity of lemongrass (Cymbopogon citratus) oil against microbes of environmental, clinical and food originEpidemiology-of-emergence-of-antimicrobial-drugs-resistance-in-bacteria-of-veterinary-clinical-importance View project Epidemiology of emergence of antimicrobial drugs resistance in bacteria of veterinary clinical importance View project.
[30] Andreu V, Mendoza G, Arruebo M, Irusta S (2015) Smart dressings based on nanostructured fibers containing natural origin antimicrobial, anti-inflammatory, and regenerative compounds. Materials 8:5154–5193
[31] Bashir S, Hina M, Iqbal J, Rajpar AH, Mujtaba MA, Alghamdi NA, Wageh S, Ramesh K, Ramesh S (2020) Fundamental concepts of hydrogels: Synthesis, properties, and their

applications. Polymers (Basel) 12:1–60
[32] Naeimi M, Tajedin R, Farahmandfar F, Naeimi M, Monajjemi M (2020) Preparation and characterization of vancomycin-loaded chitosan/PVA/PEG hydrogels for wound dressing. Mater Res Express. https://doi.org/10.1088/2053-1591/abb154
[33] Shen R, Xue S, Xu Y, Liu Q, Feng Z, Ren H, Zhai H, Kong F (2020) Research progress and development demand of nanocellulose reinforced polymer composites. Polymers (Basel). https://doi.org/10.3390/POLYM12092113
[34] Nascimento DM, Nunes YL, Figueirêdo MCB, De Azeredo HMC, Aouada FA, Feitosa JPA, Rosa MF, Dufresne A (2018) Nanocellulose nanocomposite hydrogels: Technological and environmental issues. Green Chemistry 20:2428–2448
[35] Shahzadi MP (2017) Lemon Grass (Cymbopogon citratus). Grasses - Benefits, Diversities and Functional Roles. https://doi.org/10.5772/intechopen.69518
[36] Chamkouri H (2021) A Review of Hydrogels, Their Properties and Applications in Medicine. Am J Biomed Sci Res 11:485–493
[37] Kumar Soni R, M Kewatkar S, Jain V, Singh Saluja M (2023) A Review of Hydrogels, with its Properties and Applications in Medicine. Journal of Biomedical and Pharmaceutical Research 12:20–33
[38] Rolim WR, Pieretti JC, Renó DLS, Lima BA, Nascimento MHM, Ambrosio FN, Lombello CB, Brocchi M, De Souza ACS, Seabra AB (2019) Antimicrobial Activity and Cytotoxicity to Tumor Cells of Nitric Oxide Donor and Silver Nanoparticles Containing PVA/PEG Films for Topical Applications. ACS Appl Mater Interfaces. https://doi.org/10.1021/acsami.8b19021
[39] Rafieian S, Mirzadeh H, Mahdavi H, Masoumi ME (2019) A review on nanocomposite hydrogels and their biomedical applications. IEEE Journal of Selected Topics in Quantum Electronics 26:154–174
[40] Saleem M, Saeed MT (2020) Potential application of waste fruit peels (orange, yellow lemon and banana) as wide range natural antimicrobial agent. J King Saud Univ Sci 32:805–810
[41] Yang W, Xu F, Ma X, et al (2021) Highly-toughened PVA/nanocellulose hydrogels with anti-oxidative and antibacterial properties triggered by lignin-Ag nanoparticles. Materials Science and Engineering C. https://doi.org/10.1016/j.msec.2021.112385
[42] de Lima GG, Ferreira BD, Matos M, Pereira BL, Nugent MJD, Hansel FA, Magalhães WLE (2020) Effect of cellulose size-concentration on the structure of polyvinyl alcohol hydrogels. Carbohydr Polym. https://doi.org/10.1016/j.carbpol.2020.116612
[43] Shetty SB, Mahin-Syed-Ismail P, Varghese S, Thomas-George B, Kandathil-Thajuraj P, Baby D, Haleem S, Sreedhar S, Devang-Divakar D (2016) Antimicrobial effects of Citrus sinensis peel extracts against dental caries bacteria: An in vitro study. J Clin Exp Dent 8:e71–e77
[44] Zhang J, Liu T, Liu Z, Wang Q (2019) Facile fabrication of tough photocrosslinked polyvinyl alcohol hydrogels with cellulose nanofibrils reinforcement. Polymer (Guildf) 173:103–109